INSTITUTE OF PHYSICS PUBLISHING JOURNAL OF PHYSICS D: APPLIED PHYSICS

J. Phys. D: Appl. Phys. **36** (2003) 1–9 PII: S0022-3727(03)53566-5

Optical properties of irregularly shaped particles

A A Kokhanovsky

Institute of Environmental Physics, University of Bremen, Otto Hahn Allee 1, D-28334 Bremen, Germany
and
Institute of Physics, 70 Skarina Avenue, Minsk 220072, Belarus

E-mail: alexk@iup.physik.uni-bremen.de

Received 18 September 2002, in final form 9 January 2003
Published
Online at stacks.iop.org/JPhysD/36

Abstract
The phase matrix of irregularly shaped randomly oriented large fractal particles is studied in the framework of the ray tracing approach for various refractive indices. The fractal particle model can be used for modelling local optical characteristics of various natural light scattering media with irregular particles, including oceanic water, crystalline clouds and solid aerosols. For nonabsorbing large particles the theory does not contain any fitting parameters except the refractive index of particles, which is either known (ice clouds) or has generally unknown distribution in a local volume of a scattering medium (dust aerosols and oceanic suspensions).

1. Introduction

Studies of photon transport in natural disperse media require information on their local optical characteristics (e.g. scattering and extinction matrices, Kokhanovsky (2001)). They can be easily found for the case of media with inclusions of a spherical shape (e.g. droplets in water clouds and liquid aerosols, Deirmendjian (1969)). This is not the case for most of the natural media, where particles of diverse (and irregular) shapes are often present.

An exact solution of the Maxwell's equations (of a Mie type) for an irregularly shaped particle is not possible due to the complexity of boundary conditions involved. The T-matrix approach allows for some progress (Wriedt 2002). However, it should be remembered that the solution of a light scattering problem for a single irregularly shaped particle is not very much helpful, if we need to find the response of an elementary volume of a light scattering medium with particles of irregular, but very diverse shapes. Clearly, the averaging procedure should be introduced in this case. Electromagnetic scattering calculations are usually very time consuming. So the averaging in the case of irregularly shaped particles (e.g. ice clouds or oceanic suspensions) cannot be performed numerically, considering one particle after another. Note also that the detailed information on the geometrical characteristics of irregularly shaped particles, which is needed for the averaging procedure, is usually not available.

Another possibility is to use various theoretical models, which assume that optical properties of irregularly shaped particles can be modelled using combinations of particles of simple forms (N-particle models) or by a single particle of a complex shape (1-particle model). N-particle models are studied by Liou *et al* (2000) and Kahnert *et al* (2002) among others. Different 1-particle models were developed by Shifrin and Mikulinski (1982), Peltoniemi *et al* (1989), Macke *et al* (1996), and Muinonen *et al* (1996). For the sake of completeness, we note that there are also Mie-based models of irregularly shaped particles (Chylek *et al* 1976, Pollack and Cuzzi 1980, Drossart 1990, Grenfell and Warren 1999).

The accuracy of all these models cannot be checked, using exact theory, because such a theory is not available at the moment for systems of irregularly shaped particles.

So the only possibility to find their range of validity is to compare them with experiments. Such a comparison is given here for a 1-particle model, developed by Macke *et al* (1996) for the case of randomly oriented fractal particles, which are much larger than the wavelength of incident light. We also study the dependence of the phase matrix of fractal particles on their refractive index.

2. The dependence of the phase matrix on the refractive index of fractal randomly oriented particles

2.1. General equations

Let us consider a 1-particle model, developed by Macke *et al* (1996). This is the so-called fractal particle model (FPM). In this model a system of irregularly shaped particles is substituted by a single fractal particle of a given complex shape. Then it is assumed that all essential features of light scattering by an ensemble of irregularly shaped particles are preserved in light scattering characteristics of this single particle at a random orientation.

We are interested in study of the angular distribution of scattered light intensity and polarization characteristics for ensembles of highly complex particles. By definition, these distributions should be almost featureless due to a chaotic nature of scattering in this case. These smooth distributions also arise for a single particle, but of a complex shape. However, there is no *a priori* assurance, that the model gives accurate quantitative results for a given complex light scattering medium. Therefore, the correctness of a given 1-particle model can be checked only by comparison with experiments. We make such a comparison in the next section.

Here we present results of numerical calculations of the phase matrix in the framework of the FPM. The exact structure of the irregularly shaped fractal particle (and the code used for calculation) is described elsewhere (Macke *et al* 1996).

The particle is constructed in the following way. The initial shape is a tetrahedron. A part of its triangular surface is replaced by a reduced version of the same tetrahedron. The resulting body is called the first generation of the triadic Koch fractal. Repetition of this procedure at the smaller triangles leads to higher generations. We will consider here the Koch fractals of the second generation. Optical properties of Koch fractals of the second and higher generations differ insignificantly (Macke *et al* 1996).

The interaction of light with a large fractal particle is studied in the framework of the geometrical optics, using the Monte-Carlo ray-tracing technique. Results are averaged with respect to the particle random orientation. The peak in the forward direction is described in the framework of the Fraunhofer diffraction theory (Macke *et al* 1996).

We also assume that all planes of a fractal particle have a roughness. The roughness is modelled in the following way. For each reflection–refraction event the normal of the crystal surface is tilted randomly around its original direction. The azimuth tilt angle is chosen randomly with equal distribution from the interval $[0, 2\pi]$. The zenith tilt angle is chosen from the range $[0, \pi\xi/2]$, where ξ is the roughness parameter. We assume that $\xi = 0.3$ in this study. In principle, $\xi \in [0, 1]$. It was found by Macke *et al* (1996) (see their figure 12) that larger values of ξ influence the result insignificantly.

We assume that the wavelength is $0.5\,\mu$m and the refractive index n varies in the range 1.1–1.5, which corresponds to most of the natural dispersive media in the visible region. The length D of an initial tetrahedron's side is fixed in this study and is equal to $100\,\mu$m. We also introduce the size parameter $x = kV/S \sim kD \gg 1$, where $k = 2\pi/\lambda$, V is the volume of a fractal particle and S is its surface area.

The particle is assumed to be nonabsorbing. It means that its normalized phase matrix does not depend on the size in the geometrical optics approximation (except at the small-scattering region, where Fraunhofer diffraction takes place). This makes model not very flexible as far as real experimental data (which can vary for different media) are of concern. On the other hand, there is an advantage in this. Namely, we have a fixed phase matrix for a chaotic scattering and measured matrices for various media can be checked against this simple case of a single fractal particle without introducing any fitting parameters (if the refractive index is known and there is no light absorption).

Let us describe the results obtained. For this we need to introduce the phase matrix $\hat{P}$. This matrix relates Stokes vectors of incident $\vec{S}_0(S_{01}, S_{02}, S_{03}, S_{04})$ and scattered $\vec{S}(S_1, S_2, S_3, S_4)$ light with the following matrix equation:

$$\vec{S} = \alpha \hat{P} \vec{S}_0, \tag{1}$$

where $\alpha = \sigma_{\rm sca}/4\pi r^2$, $\sigma_{\rm sca}$ is the light scattering coefficient and r is the distance from a scattering point to the observation point. We will assume that we have an ensemble of identical, but randomly oriented fractal particles. Then the matrix $\hat{P}$ takes the following general form (Kokhanovsky 2001):

$$\hat{P} = \begin{pmatrix} P_{11} & P_{12} & 0 & 0 \\ P_{12} & P_{22} & 0 & 0 \\ 0 & 0 & P_{33} & P_{34} \\ 0 & 0 & -P_{34} & P_{44} \end{pmatrix}. \tag{2}$$

Note that in contrast to the case of spherical particles $P_{22} \neq P_{11}$ and $P_{33} \neq P_{44}$. Also the parameter

$$q = \sqrt{p_{12}^2 + p_{33}^2 + p_{34}^2} \tag{3}$$

is not equal to 1 as it is the case for identical spheres. Here we introduced normalized matrix elements: $p_{ij} = P_{ij}/P_{11}$.

Equality $q = 1$ means that polarized light scattering cannot produce unpolarized light. To illustrate the physical meaning of the parameter q, we consider the illumination of a scattering medium with the phase matrix (2) by a linearly polarized light with the Stokes vector

$$\vec{S}_0 = \begin{pmatrix} 1 \\ 0 \\ 1 \\ 0 \end{pmatrix}, \tag{4}$$

which corresponds to the linear polarization at the angle 45° to a scattering plane. Then we have from equations (1), (2) and (4):

$$\vec{S} = \alpha \begin{pmatrix} P_{11} \\ P_{12} \\ P_{33} \\ -P_{34} \end{pmatrix}. \tag{5}$$

It holds for a completely polarized scattered light (Rozenberg 1955):

$$S_1^2 = S_2^2 + S_3^2 + S_4^2 \tag{6}$$

or (see equation (5))

$$P_{11}^2 = P_{12}^2 + P_{33}^2 + P_{34}^2. \tag{7}$$

Therefore, if equation (7), which is equivalent to $q = 1$, holds, the unpolarized light is not produced in a light scattering event. This is not the case for fractal particles.

Also for spheres (both polydispersed and monodispersed ones) so-called cross-polarization ratio (Kokhanovsky and Jones 2002)

$$r = \frac{1 - p_{22}}{1 - 2p_{12} + p_{22}} \tag{8}$$

is equal to zero. Note that r is equal to ratio of intensities registered for two experimental situations, namely for the case of a disperse medium placed between crossed vertical and horizontal polarizers, I_{VH}, to the case of the same medium placed between horizontal polarizers, I_{HH} (Kokhanovsky and Jones 2002). Clearly, for a spherical particle incident vertically or horizontally polarized light does not change the state of polarization due to the scattering event. It remains either vertically or horizontally polarized. So there will be no light coming from the system of spherical particles, placed between crossed polarizers. This is not the case for irregularly shaped particles (Card and Jones 1999).

Note, that both q and r do not depend on the size of particles in the framework of the geometrical optics approximation (Kokhanovsky and Jones 2002). However, they do depend on their refractive index and shape.

2.2. The phase function

Let us discuss results of numerical calculations now. The first element of the phase matrix P_{11} is given in figure 1 at various values of the refractive index n for the case of a fractal particle, described above. The dependence P_{11} on the scattering angle θ is called the phase function. It describes the conditional probability of light scattering in a fixed direction and normalized as follows:

$$\frac{1}{2}\int_0^{\pi} P_{11}(\theta) \sin\theta \, \mathrm{d}\theta = 1. \tag{9}$$

It follows from equation (9) that for isotropic scattering, when scattering does not depend on a scattering direction, we get: $P_{11} = 1$. Fractal particles with refractive index

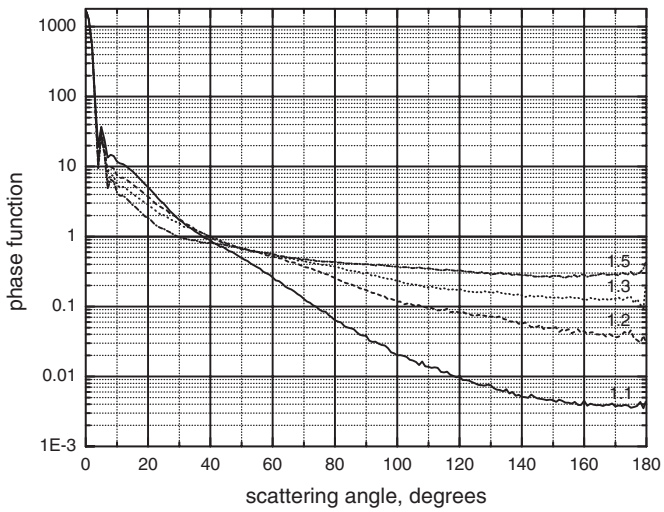

Figure 1. The phase function of fractals for various values of real part of the refractive index.

$n = 1.5$ have the phase function, which is almost isotropic in the backward hemisphere. Such phase functions were experimentally measured for dust aerosols (von Hoyningen-Huene and Posse 1997, Volten 2001, Volten *et al* 2001).

Phase functions in figure 1 are almost featureless and have smaller values for smaller n at scattering angles larger than $\pi/4$. For smaller angles ($\theta < \pi/4$), the opposite is true. Note that oscillations in figure 1 (and in figures, which follow) are due to a statistical noise of a Monte-Carlo code used.

It should be emphasized that $P_{11}(\theta)$ for systems of fractal particles considered do not depend on the refractive index of particles around $\theta \approx 45^{\circ}$ (see figure 1). Note that it may explain the existence of a cross-point at this angle for experimentally measured oceanic phase functions (Tyler 1961, Zaneveld and Pack 1973). It is known that oceanic water contains a great portion of irregularly shaped particles, having various refractive indices (Shifrin 1988, Kokhanovsky 2001). Also oceanic phase functions are featureless as those given in figure 1 (see, e.g. the case $n = 1.1$).

The case $n = 1.3$ corresponds to ice fractal particles in visible and well reproduce crystalline clouds phase functions (see, e.g. Macke *et al* (1996)). The case $n = 1.5$ roughly corresponds to dust particles (Volten 2001, Volten *et al* 2001).

The asymmetry parameter, which is defined as

$$g = \frac{1}{2}\int_0^{\pi} P_{11}(\theta) \cos\theta \sin\theta \, \mathrm{d}\theta, \tag{10}$$

was also found, using data given in figure 1 and calculations at other values of n (see table 1).

Note that this parameter can be presented in a following general form for large nonabsorbing particles (Kokhanovsky 2001):

$$g = \frac{1 + g_0}{2}, \tag{11}$$

where g_0 is the asymmetry parameter related to the geometrical optics scattering process. This process leads to almost full isotropization of photon scattering directions at large n (see figure 1). Thus, we get $g_0 \to 0$ as $n \to \infty$. This is confirmed by data given in table 1. Note that for ice crystals in the visible region ($n = 1.31$) we get $g = 0.74$, which coincides with the experimental result, obtained from measurements, performed by Garett *et al* (2001) in natural crystalline clouds (see the average asymmetry parameter in table 4 of paper by Garett *et al* (2001)). Is it only by chance or due to the possibility of

Table 1. The asymmetry parameter.

n	g_0	g
1.0	1.0	1.0
1.1	0.86	0.93
1.2	0.68	0.84
1.31	0.48	0.74
1.4	0.39	0.69
1.5	0.30	0.65
1.6	0.23	0.61
1.7	0.18	0.59
1.8	0.15	0.57
1.9	0.12	0.56
2.0	0.10	0.55
∞	0.0	0.50

the FPM to capture in a correct way light scattering by complex crystalline media, remains to be seen.

The asymmetry parameter is around 0.93 at $n = 1.1$, which is typical for oceanic hydrosols with particles having almost the same refractive index close to that of water (Shifrin 1988). Clearly, we get $g_0 \to 1$ as $n \to 1$ (see table 1).

The following parametrization holds with error less than 5% at $n \leqslant 1.9$:

$$g_0 = 0.1 + 1.2\exp(-\Upsilon(n - n_0)^2), \qquad (12)$$

where $\Upsilon = 2.65$, $n_0 = 0.68$. Equations (11) and (12) can be used for the modelling of the radiative transfer in ice clouds, using selected approximations (Kokhanovsky 2001), which do not require information on the phase function.

2.3. The normalized phase matrix

Let us consider now the normalized phase matrix elements $p_{ij} = P_{ij}/P_{11}$. We start from the element p_{12}. The degree of polarization of initially unpolarized light after scattering of light by a fractal particle is equal to $-p_{12}$. The element p_{12} is given in figure 2(*a*) for various n. It is negative for most of the angles. This means that oscillations of an electric vector are predominantly in the plane perpendicular to the scattering plane. Generally, curves in figure 2(*a*) are similar to the case of Rayleigh scattering but with strongly reduced values (e.g. it is only 5% polarization at maximum at $n = 1.5$ as opposite to the case of Rayleigh scattering, where the maximal polarization is equal to 100% at $\theta = 90^\circ$). Note also the shift of the maximum polarization angle $\theta_{\max}$ to larger angles as compared to Rayleigh scattering. Very small values of the degree of polarization and curves similar to that in figure 2(*a*) were found experimentally for oceanic water (Beardsley 1968), ice clouds (Dugin and Mirumyants 1976) and Sahara sand particles (Volten *et al* 2001). Generally, the degree of polarization decreases with n. Larger values of n lead to larger degree of randomization of photon polarization states due to a scattering event.

We see that fractal particles do not produce a strong polarization of incident unpolarized light, which is a general feature of disperse media with irregularly shaped particles.

The element p_{22} is given in figure 2(*b*). It is equal to 1 for spherical particles at any θ. So the difference $\Delta = 1 - p_{22}$ can be used as a measure of the particle's nonsphericity. We see that deviations from the spherical particle case ($p_{22} = 1$) grow with n. This result is quite understood. Namely, for optically soft particles there are almost no shape dependences of light scattering characteristics (Sid'ko *et al* 1990). Note also minima in figure 2(*b*) at $n = 1.1$ and 1.5. Such minima were observed by Voss and Fry (1984) and Volten (2001) for oceanic water and quartz aerosol particles, respectively. Generally, Δ is larger at the backward hemisphere.

The element p_{33} is given in figure 2(*c*). We see that curves $p_{33}(\theta)$ for all n (except $n = 1.5$) are close to each other around scattering angle 120°, where the value of p_{33} is small. The absolute values of p_{33} decrease with the refractive index in the forward hemisphere.

The element p_{34} is given in figure 2(*d*). It takes small negative values. This element describes the effectivity of the transformation of linear polarized light to circular polarized light for a given scattering process. Such a transformation for fractal particles has a low probability as seen from figure 2(*d*). Generally, p_{34} decreases with n.

The element p_{44} is given in figure 2(*e*). Note that the case $n = 1.1$ differs considerably from the case $n \geqslant 1.2$. The value of p_{44} describes the reduction of the degree of circular polarization for initially completely circularly polarized incident light beam.

Angular dependences $q(\theta), r(\theta)$ (see equations (3) and (8)) are given in figure 3 at $n = 1.31$ and $n = 1.5 - \mathrm{i}0.005$, which roughly correspond to ice clouds and dust aerosols, respectively. We see that the cross-polarization r by ice crystals is larger than that for dust particles in the backward hemisphere. This is mostly due to the effect of light absorption by aerosols, which diminishes the influence of the particle shape on backscattering.

The value of q is generally lower for ice crystals in the backward hemisphere. It remains smaller than 0.3 in this angular range. Remind that $q = 1$ for identical spheres. We see, therefore, that backscattering region is potentially informative for the different particulate media discrimination (Card and Jones 1999).

3. The comparison with experiments

3.1. Ice clouds

Let us compare results obtained from the FPM with experimental data, starting from the case of ice clouds. Ice clouds are composed of particles of various shapes. Their phase matrices were measured, e.g. by Dugin and Mirumyants (1976). Results of comparison of their experiments with phase matrix elements at $n = 1.3$, which is close to the refractive index of ice in the visible region, where measurements were performed, are given in figure 4. Let us analyse them.

We see that the measured and calculated functions $p_{12}(\theta)$ have similar shapes, producing a broad negative maximum at side scattering angles. The absolute values, given by the experiment and the theory, differ, however. This comes at no surprise. Indeed, the degree of polarization in measurements is obtained as a ratio $(i_1 - i_2)/(i_1 + i_2)$, where i_1 and i_2 are scattered intensities for two orthogonal polarizations. They are small and measured with estimated error up to 20%. This means that their differences, which are small numbers, can have errors exceeding 40% and more, which are not acceptable for any comparisons with the theory. Also crosses represent average over five experiments. Actual experimental data are scattered almost uniformly in the range $p_{12} \in [-0.2, 0.0]$.

The accuracy of the FPM for elements p_{33} and p_{34} is quite high, especially taking into account that no fitting parameters have been used. The sign of p_{34} was different in the experiment due to a different definition of the Stokes vector p_{34} by Dugin and Mirumyants (1976). So we multiplied experimental data for p_{34} by $j = -1$ and presented these modified data in figure 4.

Differences between calculated and measured values of p_{44} and p_{22} are quite high. However, we note again that crosses (for p_{44}) and points (for p_{22}) present only averaged data. Real experimental data are scattered around these averaged curves. The theoretical curves both for p_{44} and p_{22} are practically

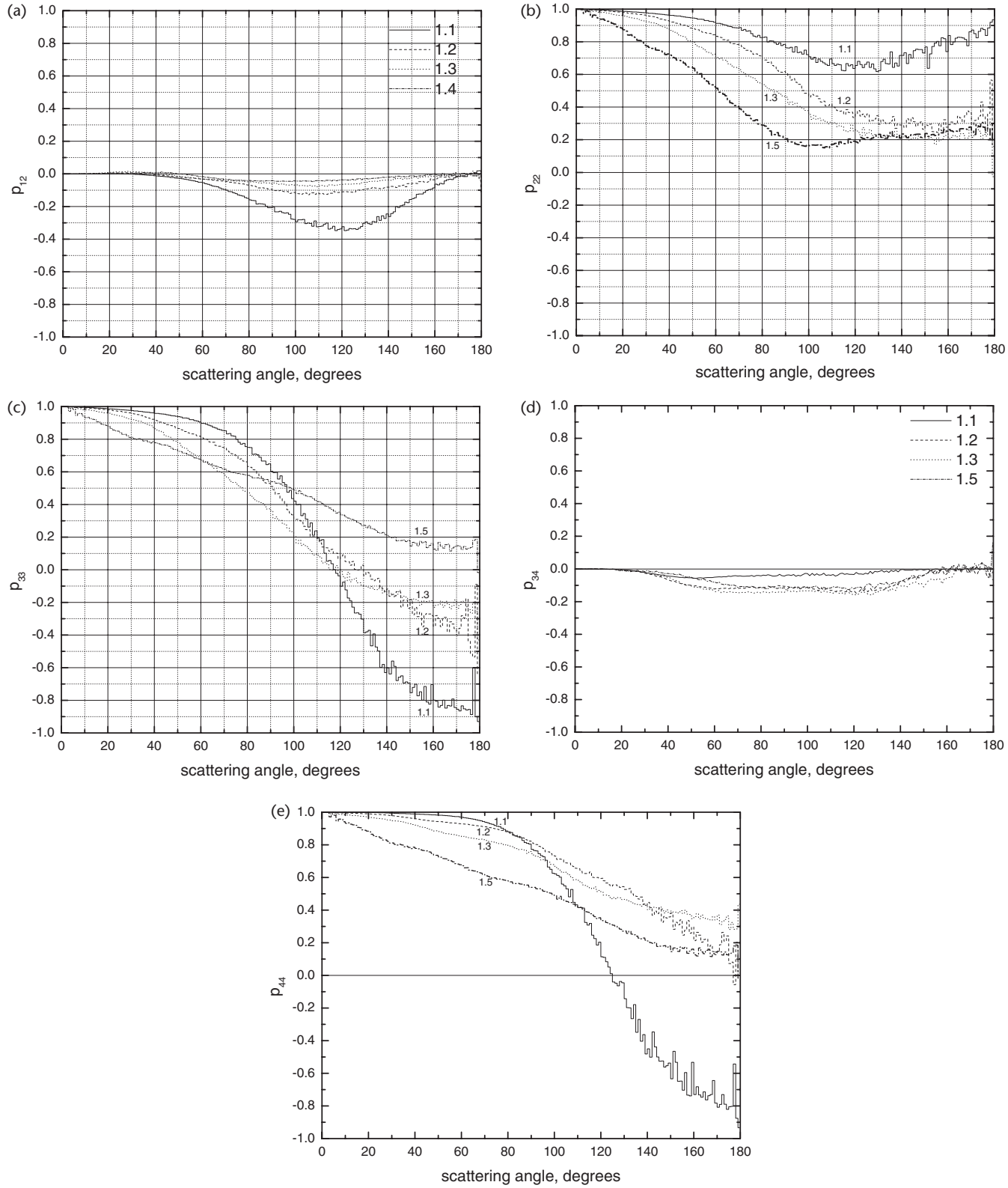

Figure 2. The same as in figure 1 but for the element p_{12} (*a*), p_{22} (*b*), p_{33} (*c*), p_{34} (*d*), p_{44} (*e*).

inside the experimental data scattering area, given by Dugin and Mirumyants (1976). Interestingly, measured values of p_{22} are closer to calculated values of p_{44} and *vice versa.* We do not have an explanation for such a peculiarity.

Overall, the FPM describes (at least qualitatively) main features of polarized light scattering by ice clouds. It can be used as input to the vector radiative transfer equation for studies of polarized radiative transfer in realistic crystalline cloudy media. Spherical particle models cannot be used in this case. Interestingly, the FPM has no fitting parameters for crystalline clouds in the visible region.

Takano and Liou (1995) compared experimental results of Dugin and Mirumyants (1976) with theoretical ray-tracing calculations, assuming the following forms of particles: solid

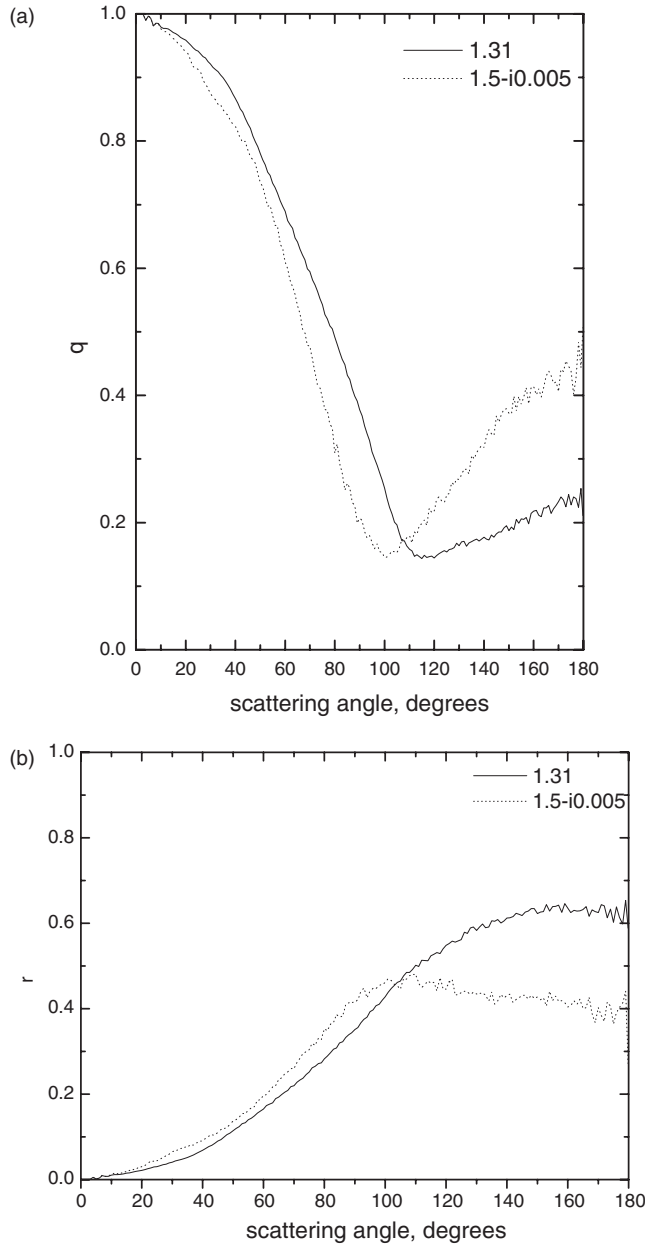

Figure 3. The dependence of parameters q (a) and r (b) on the scattering angle for ice clouds ($n = 1.3$) and dust aerosols ($n = 1.5 - \mathrm{i}0.005$), calculated in the framework of the FPM at $D = 100\,\mu$m, $\lambda = 0.5\,\mu$m.

plates and dendrites. They stated that the case of dendrites is closer to experimental data. Although, the theoretical data, given by Takano and Liou (1995) are generally closer to the experimental results than the FPM calculations presented above, their theoretical curves have special features, which are absent both in the experiment and in the results, obtained with the FPM. Thus, the FPM captures main effects of the shape irregularity on cloud polarization characteristics in a correct way as compared to modelling ice cloud particles by plates or dendrites. N-particle models (Liou *et al* 2002) can provide a better overall accuracy just because they have more fitting parameters involved. Fitting parameters are virtually absent in the FPM, however. This is the main advantage of the model, considered here.

In conclusion, we present the comparison of the phase function derived in the framework of the FPM with

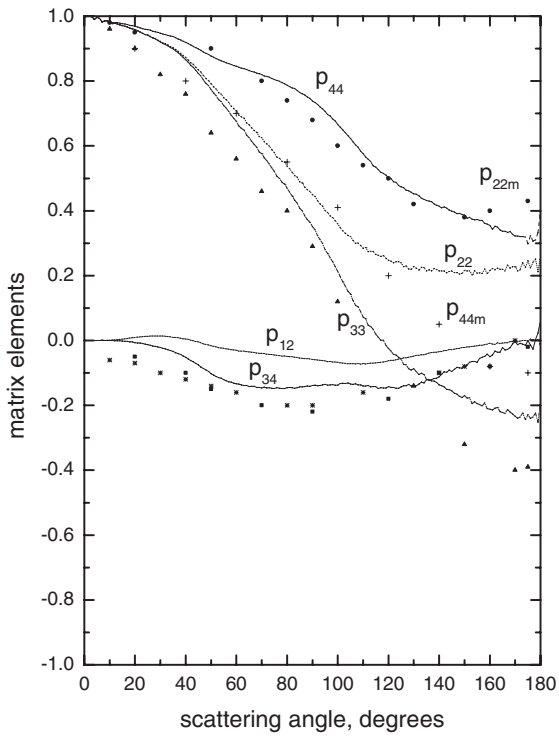

Figure 4. The comparison of calculations (lines) and measurements (●, +, ▲, ■, ∗: see paper by Dugin and Mirumyants (1976)) of the normalized matrix elements. Points and crosses give measured values $p_{22\mathrm{m}}$ and $p_{44\mathrm{m}}$, respectively. Squares and triangles correspond to measured values of p_{34} and p_{33}, respectively.

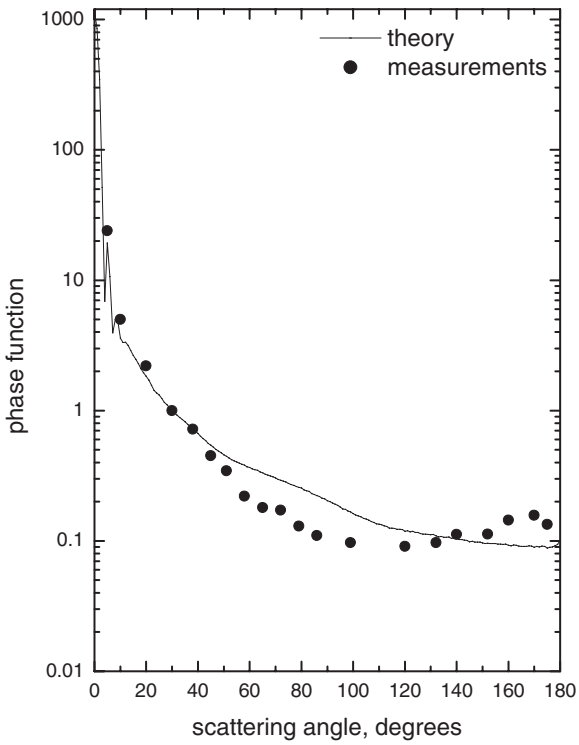

Figure 5. The phase function of an artificial crystalline cloud, obtained from measurements (Barkey and Liou 2001) and the FPM.

experimental measurements, performed by Barkey and Liou (2001) (see figure 5). The theoretical results and experimental data correspond to each other quite well. The difference can be attributed to the fact that a lot of small crystalline particles

(and, possibly, spherical droplets) were present in the chamber during the experiment. Measurements for natural clouds give featureless phase function in the backward scattering region (Baran *et al* 2001), which well corresponds to results obtained from the FPM.

We underline that due to the absence of light absorption the scattering characteristics in the visible region do not depend on the size of crystals in the framework of the geometrical optics approximation ($\lambda/D \to 0$). This explains why our model of a single particle with $D = 100\,\mu$m works quite well in the description of light scattering characteristics of crystalline clouds, characterized in reality by particle size (and shape) distributions.

3.2. Oceanic water

Oceanic water is another example of media with irregularly shaped particles (Shifrin 1988, Kokhanovsky 2001). The modelling is much more complex in this case. First of all, oceanic particles have different refractive indices (usually in the range 1.05–1.2), which complicates the analysis as opposite to the case of a well-known refractive index for ice. Also both large and small size particles play a role. Moreover, the Rayleigh scattering and *a priori* unknown light absorption by particles and water itself should be accounted for in the calculation of the phase matrix. For the sake of simplicity, we, however, neglect all these features and present results of comparison of averaged phase matrices of oceanic water (Voss and Fry 1984) with results of calculations at $n = 1.1$ in the framework of the FPM in figure 6.

We have better overall agreement of the experiment and the theory at scattering angles larger than 120°. For smaller angles, however, the difference is considerable (especially for elements p_{12} and p_{33}). Voss and Fry (1984) found that $p_{33} \approx p_{44}$ and $p_{34} \approx 0$ for oceanic water. This is consistent with a FPM as well (see figure 4).

Note that small values of p_{12} (similar to those, which follow from the FPM) are also reported in literature (Beardsley 1968). General dependences $p_{12}(\theta)$ and $p_{33}(\theta)$, obtained from the fractal model at $n = 1.1$ and the experiment, are similar, but actual values differ, which could be due to the influence of Rayleigh scattering by water and other factors, that we have mentioned in the beginning of this section. The FPM data presented in figure 6 can be used as input parameters for the theoretical vector radiative transfer studies in ocean. The advantage of this model is that it is defined by just one number (n). The correspondence of the model to experimental data can be improved, taking into account other parameters, which influence light scattering in ocean. This, however, is well outside the scope of this paper.

3.3. Quartz particles

We conclude the investigation of the validity of the FPM as compared to experiments, studying the case of yet another medium with highly irregular particles—dust aerosols. The main component of the dust aerosol over deserts is well represented by quartz aerosol particles. Measurements of phase matrices of quartz particles in the visible region were reported by Volten (2001). The comparison is given in figure 7, where we assumed that the imaginary part χ of aerosol quartz particles is equal to 0.005 and $n = 1.4$. The correspondence of the experiment and the theory is quite good for all matrix elements (except p_{44} in the forward hemisphere). Note that the value of p_{34} is positive as compared to the case of nonabsorbing aerosols (compare figures 4 and 7). So the sign of the element p_{34} (if properly defined) can serve as an indication of light absorption inside scattering particles.

The poor correspondence of the experiment and the theory for the element p_{44} can be explained by the difference of actual quartz refraction and absorption coefficients from assumed values.

Phase functions obtained from the theory and experiment (Volten *et al* 2001) for quartz particles are compared in figure 8. Again we see an excellent agreement of the FPM to the experimental data.

Volten (2001) and Volten *et al* (2001) gave also the average aerosol phase matrix, taking into account measurements of phase matrices by various samples, including Feldspar,

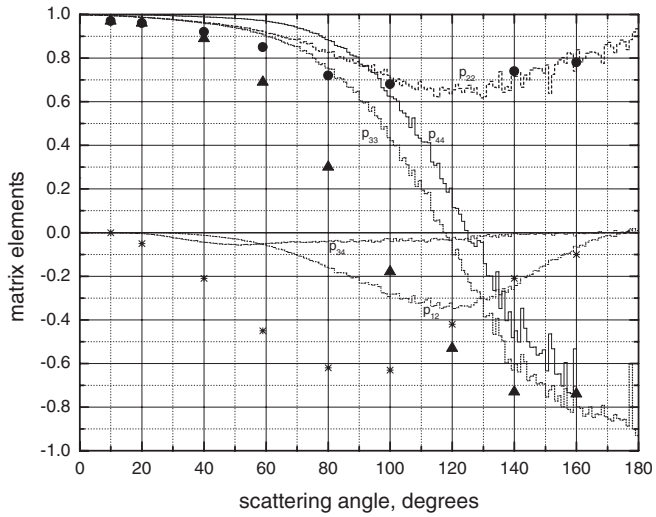

Figure 6. Normalized matrix elements, obtained from measurements (●, ▲, ∗: Voss and Fry (1984)) and calculations at $n = 1.1$ (●—p_{22}, ▲—p_{33}, ∗—p_{12}).

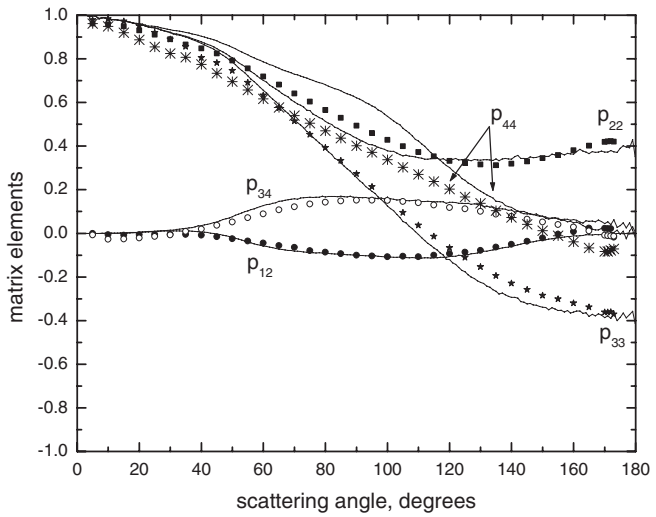

Figure 7. Normalized matrix elements, obtained from measurements (■, ★, ∗, ○, ●: Volten *et al* (2001)) and calculated ones at the complex refractive index $1.4 - i0.005$ and $D = 100\,\mu$m, $\lambda = 0.5\,\mu$m.

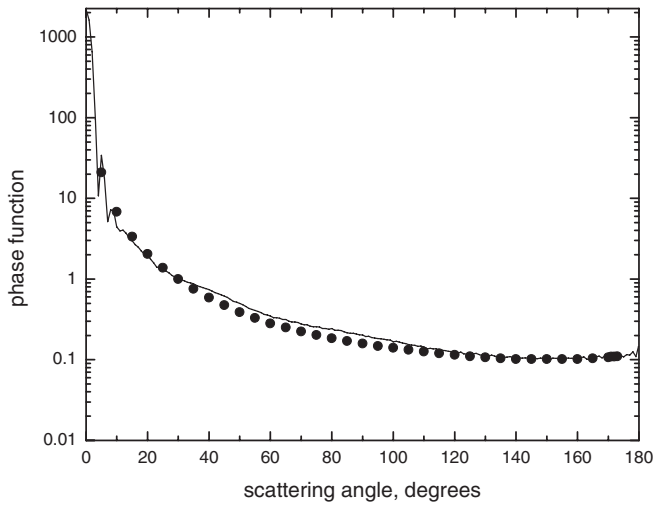

Figure 8. The phase function, normalized at the scattering angle 30°, obtained from measurements (●: Volten *et al* (2001)) and calculated at the complex refractive index $1.4 - i0.005$ and $D = 100\,\mu$m, $\lambda = 0.5\,\mu$m.

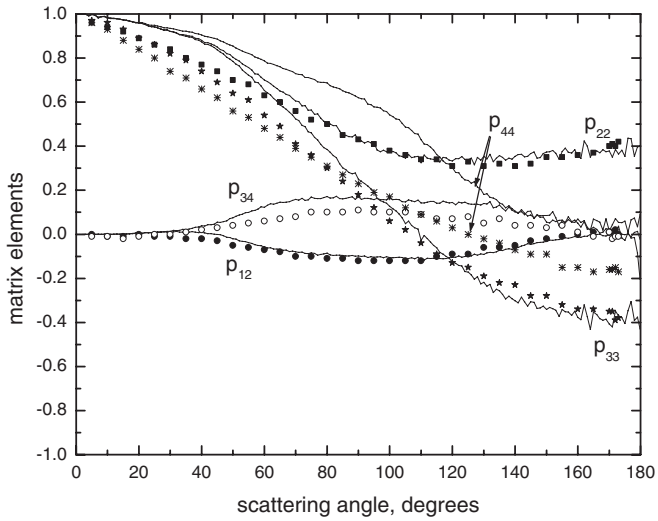

Figure 9. The same as in figure 7, but for the averaged normalized phase matrix of aerosol particles (Volten *et al* (2001)). Theoretical curves differ from those in figure 7 only due to the different statistics. We used 1000 orientations of the fractal particle for this figure as opposite to 10000 orientations of the particle in figure 7. The number of rays used was 1000 for both cases.

Red Clay, Lokon Ash, Loess, Pinatubo Ash, Quartz and Sahara dust at wavelengths 441.6 and 632.8 nm, which totals to 14 measurements. This matrix is given in figure 9 together with results obtained from the FPM, which are identical to that given in figure 7. The agreement of this average matrix model, advised for use in aerosol remote sensing problems (Volten *et al* 2001), with the FPM is rather good (again with the exception of the element p_{44}).

Phase functions obtained from the theory and averaged experimental data (Volten *et al* 2001) for the aerosol are compared in figure 10. Also we see a good agreement of the FPM and the experimental data.

This suggests that the FPM may appear to be useful in the aerosol optics studies as well. Note that Volten *et al* (2001) compared their measurements with randomized Gaussian

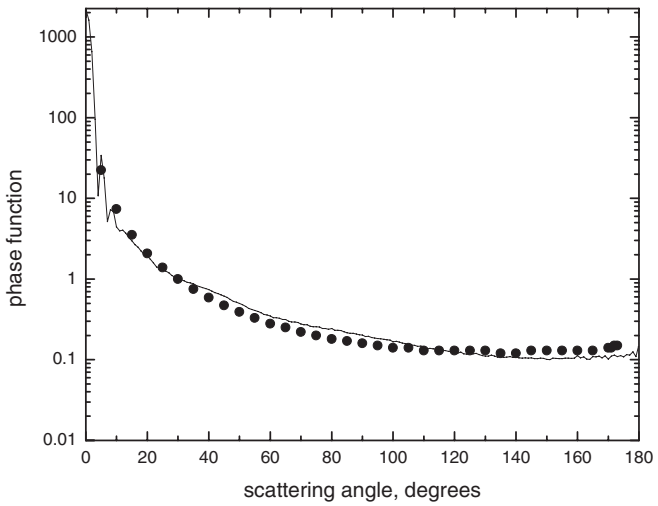

Figure 10. The same as in figure 8, but for the averaged phase function of aerosol particles (Volten *et al* 2001). The theoretical curve does not differ from that in figure 8.

particles' model (GPM). They found that the GPM describes quite well their data (although theoretical calculations give higher values of element p_{44} as compared to the measurements (see figure 13 in paper by Volten *et al* (2001)). This means that both FPM and GPM (with a special choice of parameters) give similar results. Taking into account their inherent differences, we summarize that what matters is not a particular 1-particle model, but a degree of irregularity in 1-particle model chosen.

One point should be mentioned. Aerosol particles (unlike ice crystals) can absorb light in the visible region. It means that light scattering characteristics depend on the size of particles even in the geometrical optics approximation (and generally on the particle size distribution). This may appear as a severe constraint in the value of the present analysis, which rely on calculations for a single particle with $D = 100\,\mu$m. However, in reality, what plays a major role is not a specific particle size distribution but rather a product $\Im = \chi\langle x\rangle$, where $\langle x\rangle$ is the average size parameter in the scattering ensemble of particles. This can explain a fairly good agreement we have obtained, comparing our model of a single particle (having the size parameter $x = \langle x\rangle$) with aerosol experiments. Data for the value of χ for the particles in the experiment are not available. However, we think that the value of $\Im$ used in our calculations was comparable to that in the experiment, which explains a fairly good correspondence of the experiment and numerical calculations.

4. Conclusions

In conclusion, we have studied here the dependence of the phase matrix of fractal particles on their refractive index. It was found that this model describes fairly well the light scattering by systems of large irregularly shaped particles. The theory has no fitting parameters for nonabsorbing particles, providing that the refractive index of particles is known. It means that systems of large irregularly shaped particles (as far as their optical properties are concerned) differ from one another only by the value of the refractive index in the framework of the FPM. This statement is only approximately correct, because

different particles may have different morphology, which is clearly the case for dust and ice clouds.

The model studied provides useful data for theoretical investigations of polarized light propagation in natural media, composed of irregularly shaped particles. For this one should average unphysical oscillations in curves presented above, which are due to a statistical noise of a Monte Carlo method. It can be done either increasing the number of rays/orientations or using various smoothing procedures.

The discrepancy of the theory and experiment for the element p_{44} of quartz particles should be clarified in a future research.

We hope that this paper will attract more attention to the FPM, especially with respect to atmospheric scattering studies. It is known that the Mie theory gives zero values for differences $p_{11} - p_{22}$ and $p_{44} - p_{33}$, which is not the case for irregularly shaped particles (e.g. for solid aerosols and ice crystals in the terrestrial atmosphere). Therefore, the spherical particle model cannot be applied to describe polarization characteristics of light interacting with disperse media, having a large portion of nonspherical particles (even for rapid estimates and qualitative studies). More close to reality models should be used in this case. One of such models is studied here, which is confirmed by its fairly good performance as compared to experimental data.

Acknowledgments

This work was supported by the Institute of Remote Sensing (University of Bremen). The author is grateful to A Macke for providing his Monte-Carlo code for fractal particles. He is grateful to B Barkey and H Volten for providing their experimental data in a tabular form.

References

Baran A J *et al* 2001 A scattering phase function for ice cloud: tests of applicability using aircraft and satellite multi-angle multi-wavelength radiance measurements of cirrus *Q. J. R. Meteorol. Soc.* **127** 2395–416

Barkey B and Liou K N 2001 Polar nephelometer for light—scattering measurements of ice crystals *Opt. Lett.* **26** 232–4

Beardsley G F Jr 1968 Mueller scattering matrix of sea water *J. Opt. Soc. Am.* **58** 52–7

Card J B A and Jones A R 1999 An investigation of the potential of light scattering for the characterization of irregular particles *J. Phys. D: Appl. Phys.* **32** 2466–74

Chylek P *et al* 1976 Light scattering by irregular randomly oriented particles *Science* **193** 480–2

Deirmendjian D 1969 *Light Scattering by Spherical Polydispersions* (New York: Elsevier)

Drossart P 1990 A statistical model for the scattering by irregular particles *Astrophys. J.* L39–42

Dugin V P and Mirumyants S O 1976 The light scattering matrices of artificial crystalline clouds *Izv. Acad. Sci. USSR, Atmos. Oceanic Phys.* **12** 988–91

Garrett T J *et al* 2001 Shortwave, single scattering properties of arctic ice clouds *J. Geophys. Res.* D **106** 15155–72

Grenfell T C and Warren S G 1999 Representation of a nonspherical ice particle by a collection of independent spheres for scattering and absorption of radiation *J. Geophys. Res.* D **104** 31697–709

Kahnert *et al* 2002 Using simple particle shapes to model the Stokes scattering matrix of ensembles of wavelength-sized particles with complex shape: possibilities and limitations *J. Quant. Spectrosc. Radiat. Transfer* **74** 167–82

Kokhanovsky A A 2001 *Light Scattering Media Optics: Problems and Solutions* (Berlin: Springer)

Kokhanovsky A A and Jones A R 2002 The cross-polarization of light by large nonspherical particles *J. Phys. D: Appl. Phys.* **35** 1903–6

Liou K N *et al* 2000 Light scattering and radiative transfer in ice crystal clouds: applications to climate research *Light Scattering by Nonspherical Particles* ed Mishchenko *et al* (New York: Academic) pp 418–49

Macke A *et al* 1996 Scattering properties of atmospheric ice crystals *J. Atmos. Sci.* **53** 2813–25

Muinonen K *et al* 1996 Light scattering by Gaussian random particles: ray optics approximation *J. Quant. Spectrosc. Radiat. Transfer* **55** 577–601

Peltoniemi J *et al* 1989 Scattering of light by stochastically rough particles *Appl. Opt.* **28** 4088–95

Pollack J B and Cuzzi J N 1980 Scattering by nonspherical particles of size comparable to a wavelength: a new semi-empirical theory and its application to tropospheric aerosols *J. Atmos. Sci.* **37** 868–81

Rozenberg G V 1955 Stokes vector-parameter *Uspekhi Fiz. Nauk* **56** 77–110

Sid'ko F Ya *et al* 1990 *Polarization Characteristics of Biological Suspensions* (Novosibirsk: Nauka)

Shifrin K S and Mikulinskii I A 1982 Light scattering by a system of particles in Rayleigh–Gans approximation *Opt. Spectrosc.* **52** 359–66

Shifrin K S 1988 *Introduction to Ocean Optics* (Leningrad: Gidrometeoizdat)

Takano Y and Liou K N 1995 Radiative transfer in Cirrus clouds. Part III: light scattering by irregular ice crystals *J. Atmos. Sci.* **52** 818–37

Tyler J E 1961 Measurements of scattering properties of hydrosols *J. Opt. Soc. Am.* **51** 1289–93

Volten H 2001 Light scattering by small planetary particles *PhD Thesis* (Free University: Amsterdam)

Volten H *et al* 2001 Scattering matrices of mineral particles at 441.6 and 632.8 nm *J. Geophys. Res.* D **106** 17375–401

Von Hoyningen-Huene W and Posse P 1997 Nonsphericity of aerosol particles and their contribution to radiative forcing *J. Quant. Spectrosc. Radiat. Transfer* **57** 651–68

Voss K J and Fry E S 1984 Measurement of the Mueller matrix for ocean water *Appl. Opt.* **23** 4427–39

Wriedt T 2002 Using the T-matrix light scattering computations by non-axisymmetric particles: superellipsoids and realistic shapes *Part. Part. Charact.* **19** at press

Zaneveld J R and Pack H 1973 Method for the determination of the index of refraction of particles in the ocean *J. Opt. Soc. Am.* **63** 321–4

Summary of Comments on d153566

Page: 6

Sequence number: 1
Author:
Date: 2/26/03 5:45:13 PM
Type: Note
Author: Please check the citation of figure 5

Page: 9

Sequence number: 1
Author:
Date: 2/26/03 5:45:30 PM
Type: Note
Author: Please update

Sequence number: 2
Author:
Date: 2/26/03 5:45:33 PM
Type: Highlight
Wriedt